



HHS Public Access

Author manuscript

Mol Psychiatry. Author manuscript; available in PMC 2019 February 17.

Published in final edited form as:

Mol Psychiatry. 2020 May ; 25(5): 1022–1034. doi:10.1038/s41380-018-0211-5.

Dendritic remodeling of D1 neurons by RhoA/Rho-kinase mediates depression-like behavior

Megan E. Fox¹, Ramesh Chandra¹, Miriam S. Menken¹, Emily J Larkin¹, Hyungwoo Nam¹, Michel Engeln¹, T. Chase Francis^{1,2}, Mary Kay Lobo^{1,*}

¹Department of Anatomy and Neurobiology, University of Maryland School of Medicine, Baltimore, MD, USA

Abstract

Depression alters the structure and function of brain reward circuitry. Preclinical evidence suggests that medium spiny neurons (MSNs) in the nucleus accumbens (NAc) undergo structural plasticity, however the molecular mechanism and behavioral significance is poorly understood. Here we report that atrophy of D1, but not D2 receptor containing MSNs is strongly associated with social avoidance in mice subject to social defeat stress. D1-MSN atrophy is caused by cell-type specific upregulation of the GTPase RhoA and its effector Rho-kinase. Pharmacologic and genetic reduction of activated RhoA prevents depressive outcomes to stress by preventing loss of D1-MSN dendritic arbor. Pharmacologic and genetic promotion of activated RhoA enhances depressive outcomes by reducing D1-MSN dendritic arbor and is sufficient to promote depressive-like behaviors in the absence of stress. Chronic treatment with Rho-kinase inhibitor Y-27632 after chronic social defeat stress reverses depression-like behaviors by restoring D1-MSN dendritic complexity. Taken together, our data indicate functional roles for RhoA and Rho-kinase in mediating depression-like behaviors via dendritic remodeling of NAc D1-MSNs and may prove a useful target for new depression therapeutics.

Introduction

Over 300 million people suffer from depression, exacting a global annual economic cost of \$1 trillion. Up to 40% of patient outcomes are not improved after classical antidepressants, which rely on elevating brain monoamine concentrations, take weeks to achieve efficacy, and their initial administration can increase anxiety^{1–3}. There is desperate need for new

Users may view, print, copy, and download text and data-mine the content in such documents, for the purposes of academic research, subject always to the full Conditions of use: http://www.nature.com/authors/editorial_policies/license.html#terms

*Corresponding Author: Mary Kay Lobo, 20 Penn St, HSFII Building, Rm 265, Baltimore, MD 21201, Tel: 410-706-8824, mklobo@som.umaryland.edu.

²Current address: Synaptic Plasticity Section, National Institute on Drug Abuse Intramural Research Program, Baltimore, MD, USA

Author Contributions

MEF and MKL designed the study. MEF, E.J.L., and H.N. conducted CSDS. MEF and R.C. prepared viral constructs. MEF and M.E. performed virus surgeries. MEF and M.M. conducted morphology and immunolabeling experiments. MEF and E.J.L. conducted ROCK activity and qPCR experiments. MEF conducted behavioral, pharmacologic, and RhoA activity experiments. MEF wrote the manuscript and prepared the figures with contributions from all authors. T.C.F. conducted pilot experiments that inspired the study.

Conflict of Interest

The authors have no conflict of interest to declare

antidepressants, but rational treatment development requires a detailed understanding of the neural mechanisms that cause depression. Human imaging and postmortem tissue studies have identified abnormalities in many brain regions of depressed individuals, including the nucleus accumbens (NAc)⁴⁻⁷, a key locus in brain reward circuitry. A mounting body of preclinical and clinical evidence implicates maladaptive NAc signaling in the symptomology of depression⁸⁻³¹, however the molecular underpinnings of altered NAc function in depression are poorly understood.

The primary projection neurons of the NAc are medium spiny neurons, which are divided into two subtypes based on the expression of dopamine D1 or D2 receptors (D1-MSNs and D2-MSNs, respectively)³². There is little anatomic overlap between MSN subtypes or their projection targets³³. NAc D1-MSNs send projections to the ventral tegmental area (VTA), the substantia nigra (SN), and the ventral pallidum (VP), while D2-MSNs project exclusively to the VP^{33,34}. Under normal conditions, the activity of D1- and D2-MSNs generate balanced behavioral output^{35,36}. However, biased activity of one subtype over another is hypothesized to lead to neuropsychiatric disease³⁷. Work using chronic stress models of depression has revealed opposing adaptations in MSN subtypes, where excitatory input is weakened onto D1-MSNs and strengthened onto D2-MSNs of anhedonic mice^{10,27}. Neuronal morphology is an important determinant of synaptic strength, and chronic stress induces structural plasticity in many neuronal structures³⁸⁻⁴¹ including the NAc^{23,25,42-45}. Structural adaptations in MSN subtypes may underlie the differential changes in their activity and thus warrant further investigation.

Loss of dendritic complexity is associated with neuropsychiatric disease⁴⁶, and neuronal atrophy is linked to depression in both rodent models and human patients^{43,47,48}. Recent work from our laboratory indicates D1-MSNs from stressed mice have reduced dendritic complexity²³, however the molecular mechanism behind dendritic remodeling of MSN subtypes is unknown. Further, it is unclear how dendritic arborization of specific neuron subtypes contributes to depression-like behavior. Organization of the actin cytoskeleton and neuronal morphology are modulated by small Rho family GTPases. Notably, the GTPase RhoA and its effector Rho-kinase (ROCK) play a central role in dendritic destabilization⁴⁹⁻⁵⁴. Thus, we hypothesized that RhoA would be upregulated in stressed mice and thereby contribute to the loss of dendritic arbor. Here we use neuron subtype specific translational profiling and viral-mediated molecular manipulations to show RhoA alters dendritic morphology of MSNs after chronic stress. Further, we show activated RhoA is sufficient to drive depression-like behavior in the absence of stress, and that RhoA/Rho-kinase can be targeted to rescue depressive outcomes after stress.

Materials and Methods

Experimental Subjects

All experiments were performed in accordance with the Institutional Animal Care and Use Committee guidelines at the University of Maryland School of Medicine (UMSOM). Mice were given food and water *ad libitum* and housed in UMSOM animal facilities on a 12:12 h light:dark cycle. Male hemizygous D1-Cre (Line FK150) and A2A-Cre (Line KG139) were used for morphology experiments. Homozygous RiboTag⁵⁵ mice expressing Cre-inducible

HA-Rpl22 were crossed to D1-Cre or A2A-Cre mouse lines to generate male D1-CreXRiboTag or A2A-CreXRiboTag mice and used for subtype-specific gene expression. Male and female D1-Cre mice were used for RhoA virus experiments. All mice were bred on C57BL6/J background. Male CD-1 retired breeders (Charles River, >4 months) were used as aggressors for CSDS. Male C57BL6/J mice were used for intracranial pharmacology, systemic pharmacology, and ROCK activity measurements. Mice were 8–10 weeks of age during experiments, and randomly assigned to groups unless noted.

Stereotaxic surgery

Mice were anesthetized with isoflurane (4% induction, 1.5% maintenance) and affixed in a stereotaxic frame (Kopf Instruments). For intracranial pharmacology, the scalp was removed and holes were drilled to implant an infusion cannula (Plastics One, Roanoke, VA) bilaterally over the NAc (from Bregma, AP: +1.6 mm, ML: \pm 1.5 mm; DV: -4.0 mm)⁵⁶. A dental cement skull-cap was secured with a jeweler's screw. For virus infusions, an incision was made in the scalp, and holes were drilled to target the NAc (AP+1.6mm, ML: \pm 1.5 mm, DV: -4.4 mm, 10°)²³. Cre-inducible, double inverted open (DIO) reading frame adeno-associated viruses (AAV) were infused with Neuro Syringes (Hamilton), and the scalp closed with Vet Bond (3M).

Social defeat stress

Social defeat stress was performed as previously^{15,23,27} according to well-documented procedures.⁵⁷ Briefly, mice were placed in hamster cages with perforated plexiglass dividers containing a novel, aggressive CD1-resident. For chronic social defeat stress (CSDS), mice were physically defeated by a new resident for 10 min, then housed opposite the resident for 24 hr sensory interaction for 10 consecutive days. For subthreshold social defeat stress (SSDS), mice were defeated for 3 min by 3 different residents on a single day, each session separated by 15 min of sensory interaction. 24 hr after the last defeat, social avoidance was assessed with videotracking software (CleverSys, Reston, VA, USA). Experimental mice were placed in an open field containing a perforated box. Time spent around the box ("interaction zone") was compared between two trials (2.5 min each) during which the box was empty or contained a novel CD-1. Social interaction ratios were calculated by dividing time spent in the interaction zone with and without the novel mouse present.

Immunostaining

Mice were transcardially perfused with 0.1M PBS and 4% paraformaldehyde. Brains were removed, post-fixed for 24 hr, and 100 μ m sections were collected in PBS with a vibratome (Leica, Germany). Slices were washed 3 \times 5 min with PBS and blocked in 3% normal donkey serum (NDS) and 0.3% Triton X-100 in PBS for 30 min. Slices were incubated in chicken anti-GFP (1:500; Aves Lab, Tigard, OR, USA; #GFP-1020) at 4°C overnight. Slices were washed 3 \times 5 min, then 7 \times 60 min, then incubated in Anti-Chicken Alexa 488 (1:500; Jackson Immuno, West Grove, PA, USA; #111-545-144) at 4°C overnight. Slices were washed with PBS as above, then mounted with Vectashield mounting media, and imaged on a laser-scanning confocal microscope (Olympus FV500)⁵⁶. For virus validation, 40 μ m sections were blocked as above, then incubated in chicken anti-GFP (1:4000) and rabbit anti-RhoA (1:500; New East Biosciences, King of Prussia, PA, USA; #21009) overnight at

room temperature. Slices were washed 3×10 min in PBS, then incubated for 2 hr in anti-chicken-Cy3 (1:1000, Jackson Immuno; #703-165-155) and anti-rabbit-Cy5 (1:1,000; Jackson Immuno; #711-175-152). Slices were washed in PBS, mounted with Vectashield containing DAPI, and imaged on a confocal microscope.

MSN reconstruction and dendrite analysis

D1-Cre or A2A-Cre mice were injected with AAV5-Ef1a-DIO-eYFP (UNC Vector Core, Chapel Hill, NC, USA, diluted to 1.5×10^{11} VP/mL). Sections containing NAc were sampled from bregma AP:1.5–1.0 mm and Z-stack images were acquired at 0.6 μ m increments using a 40x objective. MSNs were 3D reconstructed using Imaris 8.3 software (Bitplane, Oxford Instruments) as described previously⁵⁶. Surfaces were masked to generate a 2D image of a single MSN for sholl analysis. Concentric ring intersections were determined using the ImageJ sholl analysis plugin⁵⁸ at 10 μ m increments from soma.

RNA isolation

Polyribosomes were immunoprecipitated from NAc of D1-Cre-RiboTag and A2A-Cre-RiboTag mice as described previously⁵⁹. Briefly, four 14-gauge NAc tissue punches per mouse (4 mice pooled/sample) were collected 24 hr after social interaction. Tissue punches were homogenized by douncing in 1 mL homogenization buffer, and the supernatant was incubated with 5 μ l anti-HA antibody (Covance, Princeton, NJ, USA: #MMS-101 R) at 4°C overnight with constant rotation. Samples were then incubated with 400 μ l of protein G magnetic beads (Life Technologies, Carlsbad, CA, USA #100.09D) overnight at 4°C with constant rotation. Beads were washed in a magnetic rack with high-salt buffer. RNA was extracted with a DNase step (Qiagen, Germantown, MD, USA) using the MicroElute Total RNA Kit (Omega, Norcross, GA, USA) by adding TRK lysis buffer, and following the manufacturer's instructions. RNA was quantified with a NanoDrop (Thermo Scientific), and 300–400 ng of cDNA was synthesized with iScript cDNA synthesis kit (Bio-Rad, Hercules, CA, USA). cDNA expression changes were measured using qRT-PCR with Perfecta SYBR Green FastMix (Quanta, Beverly, MA, USA) using the $-CT$ method described previously⁶⁰ compared to GAPDH. Primer sequences can be found in Supplementary Table 1.

ROCK Activity

Two 14-gauge NAc tissue punches were collected in 0.1M PBS containing protease inhibitors (Roche, Mannheim, Germany). Punches were homogenized on ice in 30 μ l of lysis buffer (50 mM Tris-HCl, 150 mM NaCl, 1 mM EDTA, 1% Triton-X100) supplemented with protease (Sigma P8340) and phosphatase inhibitors (Sigma P5726 and P0044) using an ultrasonic processor (Cole Parmer, Vernon Hills, IL, USA). Samples were centrifuged (4°C, 13000 RPM, 10 min), and protein concentrations were normalized with homogenization buffer. ROCK activity was determined using an ELISA (EMD Millipore, Burlington, MA, USA, #CSA001) according to the manufacturer's instructions.

Activated RhoA

Activated RhoA was determined with a RhoA activation G-LISA (Cytoskeleton # BK124, Denver, CO, USA) using materials provided in the kit. Three 14-gauge NAc tissue punches were homogenized with a Pellet Pestle (Thermo Fisher) in 100 μ l lysis buffer. Homogenates were centrifuged (4°C, 13000 RPM, 1 min), and supernatants snap-frozen at -80°C for later processing. Lysates were thawed on ice, and protein concentrations were equalized with ice cold lysis buffer before following manufacturer's instructions.

Intracranial Pharmacology

Cell-permeable C3-transferase (#CT04) and Rho Activator II (#CN03) were obtained from Cytoskeleton, suspended in sterile water (100 μ g/mL), and diluted to 10 μ g/mL in 0.9% saline. Drugs were delivered 500 nL/side over 10 min, 4 hours prior to the stress episode.

Cell-type specific RhoA manipulation

Plasmids encoding AAV2.2-Ef1a-DIO-RhoAT19N-eYFP and AAV2.2-Ef1a-DIO-RhoA-eYFP were constructed from pcDNA3-RhoAT19N and pcDNA3RhoA plasmids⁶¹ (Addgene #12967, #12965), PCR amplified, and ligated into an Ef1a-DIO-eYFP vector. Vector sequences were confirmed by digestion and sequencing, and packaged as described previously⁵⁹. At 5–6 weeks of age, D1-Cre mice underwent stereotaxic surgery for intra-NAc infusion of RhoA vectors, given 3 weeks for recovery and expression, and housed in groups of 4–5 before behavioral testing or stress.

Behavioral Testing

Mice were subject to a battery of 5 behavioral tests over 5 days. For Splash, mice were habituated to an empty cylinder, then their dorsal coat surface sprayed 3 times with 10% sucrose. Time spent grooming was recorded over 5 min and scored by a blinded experimenter⁶². For elevated plus maze, mice were placed in the center of the maze and their activity in open and closed arms was recorded over 5 min with video tracking software. For open field, mice were placed in the center of the open field, and time spent in the center and total distance moved were recorded over 15 min with video tracking software. For sucrose preference, mice were housed individually after open field and given two 50 mL conical tubes with sipper tops containing water or 1% sucrose²⁷. Tube position was rotated daily to account for side preference, and preference for sucrose over water was determined over 2 consecutive days by weighing the tubes and comparing water vs sucrose consumption. For forced-swim, mice were placed in a cylinder of room temperature water, and time immobile was recorded over 6 min and scored by a blinded experimenter.

Systemic Rho-kinase inhibition

After CSDS, mice were assigned a treatment group (vehicle or Y-27632) based on individual social interaction ratio such that each group contained a similar distribution of social interaction ratios. Mice were pair-housed across a perforated divider with a similar scoring mouse for the duration of treatment (Day 12–18), and individually housed prior to the second social interaction test (end of day 18). Y-27632 (5 mg/kg) (Tocris, Ellisville, MO, USA) or vehicle (saline) were administered s.c. (4 mL/kg) once daily for 7d.

Statistics

Mice with off-target injection sites were excluded from analysis. Data are presented as mean \pm sem with individual data points overlaid. All statistical tests were performed in Graph Pad Prism 6.0. A detailed table of all statistical analysis is in Supplementary Table 2. Sample sizes were determined with GraphPad Statmate 2.0, using standard deviations from previous experiments and significance level (α)=0.05.

Results

Stress causes dendritic atrophy and RhoA GTPase upregulation selectively in NAc D1-MSNs

Previous work indicates stress-susceptible mice have reduced D1-MSN dendritic complexity. To determine if dendritic atrophy is exclusive to D1-MSNs, we used a low-titer Cre-dependent AAV-eYFP in D1- and A2A-Cre mice (the latter display expression of Cre in D2-MSNs but not cholinergic interneurons unlike the D2-Cre line⁶³) to sparsely label D1 or D2 MSNs in mice subjected to chronic social defeat stress (CSDS; Figure 1a, b, behavior in Supplementary Figure 1a, c). In agreement with our previous study²³, we found D1-MSNs from CSDS mice had reduced dendritic complexity (Sholl intersections, $P<0.0001$; number of branch points $P=0.0003$, Figure 1c–e), and total dendritic length ($P=0.0006$; Figure 1e), but unaltered soma volume (Supplementary Figure 1a). D2-MSN complexity, dendritic length, and soma volume were unaltered in stressed mice ($P>0.05$, Figure 1f–h, Supplementary Figure 1c). Neither D1- nor D2-MSNs from the dorsal striatum had reduced dendritic complexity, suggesting stress-induced atrophy is specific D1-MSNs in the NAc (Supplementary Figure 2). To strengthen the link between dendritic complexity of NAc MSNs and depression-like behavior, we compared the area under the sholl profile and social interaction behavior for individual mice. We found a linear relationship between sholl profile and social interaction for D1- ($P=0.0168$; Figure 1c) but not D2-MSNs ($P=0.2858$, Figure 1f). To examine possible molecular mechanisms of D1-MSN selective atrophy, we used neuron subtype-specific translational profiling to screen for altered small GTPase expression (Figure 1i). We found RhoA and its downstream effector, Rho-kinase (ROCK) were upregulated exclusively in D1 MSNs of CSDS mice, while other GTPases were unchanged (*Rhoa* D1: $P=0.0008$, *Rock2* D1: $P=0.0031$, Figure 1j, behavior in Supplementary Figure 1b, d, other GTPases Supplementary Figure 3). Rho Guanine Nucleotide Exchange Factor 1 was also upregulated exclusively in D1-MSNs of stressed mice (*Arhgef1* D1: $P=0.0067$, Figure 1j), and Rhotekin, an inhibitor of GTPase activity, was downregulated in D1-MSNs (*Rtkn* D1: $P=0.0150$, Figure 1j). ROCK activity was also increased in total NAc of CSDS mice ($P<0.0001$, Figure 1k, behavior in Supplemental Figure 1e). RhoA upregulation was specific to NAc MSNs, since analysis of whole dorsal striatum tissue revealed RhoA was unchanged and ROCK2 was downregulated in CSDS mice (Supplementary Figure 1f).

NAc RhoA controls susceptibility to social defeat stress

RhoA plays a key role in dendritic destabilization, and its upregulation in NAc D1-MSNs likely contributes to the dendritic atrophy associated with social avoidance. Thus, we next asked if inhibiting NAc RhoA could prevent depression-like behavior after stress. We implanted mice with cannulas targeting the NAc and inhibited RhoA during CSDS with a

cell-permeable C3-transferase (C3T, Figure 2a). Mice treated with C3T had higher social interaction ratios than those treated with vehicle ($P=0.0170$; Figure 2b–c) that were not due to locomotor effects ($P>0.05$, Figure 2c). RhoA inhibition did not alter social interaction of control mice ($P>0.05$, Figure 2c), and reduced GTP-bound, activated RhoA in CSDS mice ($P=0.0010$, Figure 2d). Since RhoA inhibition prevented the social avoidance outcome to stress, we next asked if increasing activated RhoA would promote susceptibility to a subthreshold stress. Mice were given intra-NAc Rho activating compound CN03 and subjected to a 1-day subthreshold social defeat stress (SSDS, Figure 2e). SSDS does not normally result in depression-like behavior, however mice treated with CN03 had reduced social interaction ratios as compared with vehicle ($P=0.0082$, Figure 2f–g), that were not due to locomotor effects ($P>0.05$, Figure 2g). CN03 treatment increased GTP-bound, activated RhoA (Control, $P=0.0364$; SSDS, $P=0.0101$, Figure 2h), however only stressed mice showed reduced social interaction behavior.

RhoA acts in D1-MSNs to reduce dendritic complexity and social interaction after stress

Since modulating RhoA in the NAc influenced susceptibility to social defeat stress, we next asked if RhoA specifically in D1-MSNs was sufficient to generate depressive outcomes to stress. We developed Cre-inducible adeno-associated viruses (AAVs) to over-express RhoA (WT-RhoA), or a dominant negative (RhoAT19N; DN-RhoA) mutant⁶¹ (Figure 3a). We validated our constructs using immunofluorescence (example in Figure 3b) and by measuring GTP bound, activated RhoA in NAc tissue lysates from mice expressing the vectors. Expression of the dominant negative mutant decreased activated, GTP-bound RhoA by 39%, whereas overexpression of wildtype RhoA increased activated RhoA by 213% compared to eYFP (eYFP vs DN-RhoA: $P=0.0016$; eYFP vs WT-RhoA $P=0.0105$; Figure 3c). We next expressed DN-RhoA in D1-MSNs to block activated RhoA during CSDS (Figure 3d). CSDS mice expressing DN-RhoA had higher social interaction ratios compared to eYFP CSDS mice, suggesting DN-RhoA prevented the induction of stress susceptibility ($P=0.0042$ Figure 3e), and to a similar extent as pharmacological RhoA inhibition in the NAc. When we examined the morphology of D1-MSNs expressing DN-RhoA, we found greater dendritic complexity (Sholl intersections, $P<0.0001$, Figure 3f, h) that correlated with social interaction behavior ($P=0.0238$, Figure 3g). DN-RhoA D1-MSNs on average had greater total dendritic length and number of branch points, although this did not reach statistical significance (Length, $P=0.1445$, Branch points $P=0.1783$, Figure 3i). To determine if increasing activated RhoA specifically in D1-MSNs could enhance susceptibility to subthreshold stress, we expressed WT-RhoA prior to SSDS (Figure 3j). WT-RhoA decreased social interaction ratio compared to eYFP ($P=0.0021$, Figure 3k) in a similar manner to total NAc RhoA activation. When we examined the morphology of D1-MSNs, WT-RhoA caused a marked decrease in dendritic complexity (Sholl intersections, $P=0.0021$, Figure 3l, n) that correlated with social interaction (Figure 3m) and reduced total dendritic length ($P=0.0116$, Figure 3o). Soma volumes were not different between any MSNs (Supplementary Figure 4). Given that pharmacologic activation of RhoA enhanced susceptibility to subthreshold stress, we also expressed WT-RhoA in D2-MSNs prior to SSDS (Supplementary Figure 5). Driving RhoA activity in D2-MSNs did not decrease social interaction compared to eYFP ($P>0.05$, Supplementary Figure 5), suggesting that the pro-susceptibility effects of RhoA are specific to D1-MSNs.

RhoA in D1-MSNs alters dendritic complexity and enhances depression-like behavior in stress naïve mice

Since activated RhoA in D1-MSNs drove depressive outcomes after stress, we next asked if RhoA could influence dendritic complexity and depression-like behaviors in the absence of stress. We injected male and female D1-Cre mice with our RhoA constructs and assessed baseline depression- and anxiety-like behavior (Figure 4a). WT-RhoA reduced dendritic complexity in stress-naïve mice ($P < 0.0001$, Figure 4b–c), decreased total dendritic length (eYFP vs. WT-RhoA, $P = 0.0003$; DN-RhoA vs. WT-RhoA, $P = 0.0261$) and decreased number of branch points (eYFP vs. WT-RhoA, $P = 0.0475$; DN-RhoA vs. WT-RhoA, $P = 0.0103$) without altering soma volume ($P > 0.05$, Figure 4d). WT-RhoA in D1-MSNs was sufficient to increase depression-like behavior without stress: female mice spent less time grooming in the splash test ($P = 0.0084$), male mice had decreased sucrose preference ($P = 0.0254$), and both sexes spent more time immobile in the forced swim test (Male, $P = 0.0294$; Female, $P = 0.0035$, Figure 4e). D1-MSN RhoA manipulation had no effect on anxiety-like behavior in the elevated plus maze or open field, nor did it alter locomotion in either sex ($P > 0.05$, Figure 4f).

Inhibition of downstream effector Rho-kinase reverses depressive outcomes to stress and dendritic atrophy

We next sought to reverse depressive outcomes to stress by targeting the primary effector of RhoA, Rho-kinase (ROCK). Mice underwent CSDS, were tested for social interaction behavior, and were then treated systemically with the ROCK inhibitor Y27632 (5 mg/kg s.c., Y27, Figure 5a). Seven days of Y27 treatment increased social interaction time in CSDS mice ($P = 0.0182$, Figure 5b–c) without altering behavior of control mice. Y27-treated CSDS mice had decreased active ROCK compared to vehicle-treated ($P = 0.0204$, Figure 5d) and more closely resembled control mice. Acute Y27 treatment did not alter social interaction behavior of CSDS mice (Supplementary Figure 6), suggesting chronic treatment is necessary for its antidepressant actions. To determine if ROCK inhibition improved social interaction behavior by altering dendritic complexity, we labeled D1-MSNs using eYFP as before (Figure 5e). Mice treated with Y27 after CSDS had increased D1-MSN dendritic complexity ($P < 0.0001$, Figure 5f–g) that correlated with social interaction behavior ($P = 0.0183$ Figure 5h), increased dendritic length ($P = 0.0041$) and number of branch points ($P = 0.0076$), but no change in soma volume ($P > 0.05$, Figure 5i). To ensure the antidepressant effect of Y27 treatment was not restricted to social interaction, we also tested immobility time in the forced swim test. Y27 treated mice spent less time immobile as compared to vehicle treated mice. ($P = 0.0265$, Figure 5j).

Discussion

This work establishes that chronic stress selectively induces dendritic atrophy of D1-MSNs in the NAc via increased RhoA pathway activation. First, RhoA is increased in D1-MSNs after chronic stress and enhancing RhoA recapitulates both the behavioral and morphological changes found in stressed mice. Second, blocking RhoA activation in D1-MSNs attenuates dendritic atrophy and social avoidance after chronic stress. Third, activated RhoA in D1-MSNs contributes to depression-like behavior in the absence of stress by

altering D1-MSN morphology. Finally, inhibition of downstream target Rho-kinase reverses depressive outcomes to stress by restoring dendritic arbor of D1-MSNs.

Volume and dendritic complexity are reduced in the brains of depressed patients and animal models.^{43,46–48} Here we established that in the NAc, dendritic atrophy is specific to D1-MSNs and driven by RhoA. Loss of D1-MSN arbor is consistent with the loss of synaptic drive onto D1-MSNs after stress, which is thought to generate anhedonia.^{10,27} Spine density on D1-MSNs is unchanged in stressed mice²³, which is consistent with the effects of psychosocial stress on hippocampal CA3 neurons which exhibit atrophy without altered spine density.⁶⁴ However, it is still unclear if spine changes precede the loss of dendritic arbor in either cell population. In hippocampal neurons, spine loss can occur within hours after stress⁶⁵. Further, spine loss induced by the stress hormone corticotropin releasing factor (CRF) is driven by RhoA⁶⁶. It is thus plausible that in the NAc, as inputs are decreased onto D1-MSNs, RhoA first causes spine loss on vulnerable dendrites prior to their atrophy. To understand the precise mechanisms of dendritic remodeling in stress, future experiments should determine which excitatory inputs are reduced onto D1-MSNs, and what makes specific dendritic segments vulnerable to atrophy. Nevertheless, it is clear reduced arborization of D1-MSNs via activated RhoA plays a significant role in depression and stress-related behaviors.

NAc MSNs undergo structural plasticity after stress, but D1- and D2-MSNs exhibit opposing electrophysiologic adaptations²⁷. The cell-type specificity of stress-induced plasticity, together with D1-MSN specific atrophy indicates there are unique molecular mechanisms governing adaptations in D1- and D2-MSNs in stress-related behaviors. Here, we showed D1-MSN atrophy is caused by neuron subtype specific upregulation of the RhoA pathway. This D1-specific upregulation can likely be attributed to differences in upstream molecular regulators of RhoA expression. One such regulator is the transcription factor Egr3,²³ which can regulate RhoA expression, and is increased in D1-, but not D2-MSNs of stressed mice.²³ Since D2-MSNs did not undergo dendritic atrophy, but have enhanced excitatory input after chronic stress²⁷, it is tempting to speculate spine density is increased on D2-MSNs. In agreement with this, I κ B kinase and Rac1 increase spine density on MSNs to regulate depressive outcomes to stress^{25,44} Since spine density is unchanged on D1-MSNs²³, we believe the spine changes described in these studies^{25,44} are occurring mainly in D2-MSNs. Future experiments should confirm that changes to dendritic spines in the NAc can be attributed to D2-MSNs, and identify the molecular mechanisms responsible for this cell-type specific adaptation.

Rho-kinase inhibitors can inhibit habitual responding for cocaine,⁶⁷ prevent behavioral despair caused by restraint stress⁶⁸, and are used to treat other disease states in humans^{69,70} Here, we identified new antidepressant actions of the Rho-kinase inhibitor Y-27632. Remarkably, treatment with Y-27632 restored dendritic complexity of D1-MSNs and improved both social interaction and forced swim behaviors. Classical antidepressants can take several weeks to achieve efficacy, whereas our treatment was effective after 7 days. Although not rapidly acting like ketamine, Rho-kinase inhibitors do not likely have its abuse liability. Rho-kinase inhibitors may also be useful compounds for treating other disease states characterized by loss of dendritic arbor.

In summary, we provide strong evidence that chronic stress induces upregulation of RhoA to drive loss of D1-MSN dendritic complexity. RhoA-dependent atrophy promotes depressive behaviors that can be pharmacologically reversed, suggesting RhoA and ROCK inhibitors may prove useful as novel antidepressant compounds.

Supplementary Material

Refer to Web version on PubMed Central for supplementary material.

Acknowledgments

This work was funded by a One Mind/Janssen Rising Star Translational Research Award (MKL), NIH R01MH106500 (MKL) and NIH F32MH116574 (MEF).

References

- Marcinkiewicz CA, et al. Serotonin engages an anxiety and fear-promoting circuit in the extended amygdala. *Nature*. 537:97–101.2016; [PubMed: 27556938]
- Belzung C, Le Guisquet AM, Barreau S, Calatayud F. An investigation of the mechanisms responsible for acute fluoxetine-induced anxiogenic-like effects in mice. *Behav Pharmacol*. 12:151–62.2001; [PubMed: 11485052]
- Holtzheimer PE, Mayberg HS. Stuck in a rut: rethinking depression and its treatment. *Trends Neurosci*. 34:1–9.2011; [PubMed: 21067824]
- Zhu MY, et al. Elevated levels of tyrosine hydroxylase in the locus coeruleus in major depression. *Biol Psychiatry*. 46:1275–1286.1999; [PubMed: 10560033]
- Liotti M, Mayberg HS. The Role of Functional Neuroimaging in the Neuropsychology of Depression. *J Clin Exp Neuropsychol (Neuropsychology, Dev Cogn Sect A)*. 23:121–136.2001;
- Drevets WC. Neuroimaging and neuropathological studies of depression: implications for the cognitive-emotional features of mood disorders. *Curr Opin Neurobiol*. 11:240–249.2001; [PubMed: 11301246]
- Nestler EJ, et al. Neurobiology of depression. *Neuron*. 34:13–25.2002; [PubMed: 11931738]
- Floresco SB. The Nucleus Accumbens: An Interface Between Cognition, Emotion, and Action. *Annu Rev Psychol*. 66:25–52.2015; [PubMed: 25251489]
- Russo SJ, Nestler EJ. The brain reward circuitry in mood disorders. *Nat Rev Neurosci*. 14:609–625.2013; [PubMed: 23942470]
- Lim BK, Huang KW, Grueter BA, Rothwell PE, Malenka RC. Anhedonia requires MC4R-mediated synaptic adaptations in nucleus accumbens. *Nature*. 487:183–189.2012; [PubMed: 22785313]
- Chaudhury D, et al. Rapid regulation of depression-related behaviours by control of midbrain dopamine neurons. *Nature*. 493:532–6.2013; [PubMed: 23235832]
- Wilkinson MB, et al. A Novel Role of the WNT-Dishevelled-GSK3 β Signaling Cascade in the Mouse Nucleus Accumbens in a Social Defeat Model of Depression. *J Neurosci*. 31:2011;
- Vialou V, et al. DeltaFosB in brain reward circuits mediates resilience to stress and antidepressant responses. *Nat Neurosci*. 13:745–52.2010; [PubMed: 20473292]
- Kim HD, et al. SIRT1 Mediates Depression-Like Behaviors in the Nucleus Accumbens. *J Neurosci*. 36:8441–8452.2016; [PubMed: 27511015]
- Chandra R, et al. Reduced Slc6a15 in nucleus accumbens D2-neurons underlies stress susceptibility. *J Neurosci*. :3250–16.2017; DOI: 10.1523/JNEUROSCI.3250-16.2017
- Pizzagalli DA, et al. Reduced Caudate and Nucleus Accumbens Response to Rewards in Unmedicated Individuals With Major Depressive Disorder. *Am J Psychiatry*. 166:702–710.2009; [PubMed: 19411368]

17. Smoski MJ, et al. fMRI of alterations in reward selection, anticipation, and feedback in major depressive disorder. *J Affect Disord.* 118:69–78.2009; [PubMed: 19261334]
18. Stoy M, et al. Hyporeactivity of ventral striatum towards incentive stimuli in unmedicated depressed patients normalizes after treatment with escitalopram. *J Psychopharmacol.* 26:677–688.2012; [PubMed: 21926423]
19. Robinson OJ, Cools R, Carlisi CO, Sahakian BJ, Drevets WC. Ventral Striatum Response During Reward and Punishment Reversal Learning in Unmedicated Major Depressive Disorder. *Am J Psychiatry.* 169:152–159.2012; [PubMed: 22420038]
20. Krishnan V, et al. Molecular Adaptations Underlying Susceptibility and Resistance to Social Defeat in Brain Reward Regions. *Cell.* 131:391–404.2007; [PubMed: 17956738]
21. Misaki M, Suzuki H, Savitz J, Drevets WC, Bodurka J. Individual Variations in Nucleus Accumbens Responses Associated with Major Depressive Disorder Symptoms. *Sci Rep.* 6:21227.2016; [PubMed: 26880358]
22. Heshmati M, et al. Cell-type-specific role for nucleus accumbens neuroligin-2 in depression and stress susceptibility. *Proc Natl Acad Sci U S A.* 115:1111–1116.2018; [PubMed: 29339486]
23. Francis TC, et al. Molecular basis of dendritic atrophy and activity in stress susceptibility. *Mol Psychiatry.* 22:1512–1519.2017; [PubMed: 28894298]
24. Muir J, et al. In Vivo Fiber Photometry Reveals Signature of Future Stress Susceptibility in Nucleus Accumbens. *Neuropsychopharmacology.* 2017; doi: 10.1038/npp.2017.122
25. Golden SA, et al. Epigenetic regulation of RAC1 induces synaptic remodeling in stress disorders and depression. *Nat Med.* 19:337–344.2013; [PubMed: 23416703]
26. Christoffel DJ, et al. Effects of Inhibitor of κ B Kinase Activity in the Nucleus Accumbens on Emotional Behavior. *Neuropsychopharmacology.* 37:2615–2623.2012; [PubMed: 22781845]
27. Francis TC, et al. Nucleus accumbens medium spiny neuron subtypes mediate depression-related outcomes to social defeat stress. *Biol Psychiatry.* 77:212–222.2015; [PubMed: 25173629]
28. Wook Koo J, et al. Essential Role of Mesolimbic Brain-Derived Neurotrophic Factor in Chronic Social Stress–Induced Depressive Behaviors. *Biol Psychiatry.* 80:469–478.2016; [PubMed: 26858215]
29. Sun H, et al. ACF chromatin-remodeling complex mediates stress-induced depressive-like behavior. *Nat Med.* 21:1146–1153.2015; [PubMed: 26390241]
30. Covington HE, et al. Antidepressant actions of histone deacetylase inhibitors. *J Neurosci.* 29:11451–60.2009; [PubMed: 19759294]
31. Dias C, et al. β -catenin mediates stress resilience through Dicer1/microRNA regulation. *Nature.* 516:51–5.2014; [PubMed: 25383518]
32. Gerfen CR, Surmeier DJ. Modulation of Striatal Projection Systems by Dopamine. *Annu Rev Neurosci.* 34:441–466.2011; [PubMed: 21469956]
33. Kupchik YM, et al. Coding the direct/indirect pathways by D1 and D2 receptors is not valid for accumbens projections. *Nat Neurosci.* 18:1230–1232.2015; [PubMed: 26214370]
34. Villalba RM, Smith Y. Differential striatal spine pathology in Parkinson’s disease and cocaine addiction: a key role of dopamine? *Neuroscience.* 251:2–20.2013; [PubMed: 23867772]
35. Gerfen CR. The neostriatal mosaic: multiple levels of compartmental organization in the basal ganglia. *Annu Rev Neurosci.* 15:285–320.1992; [PubMed: 1575444]
36. Nicola SM. The nucleus accumbens as part of a basal ganglia action selection circuit. *Psychopharmacology (Berl).* 191:521–50.2007; [PubMed: 16983543]
37. Maia TV, Frank MJ. From reinforcement learning models to psychiatric and neurological disorders. *Nat Neurosci.* 14:154–62.2011; [PubMed: 21270784]
38. Fuchs E, Flugge G, Czeh B. Remodeling of neuronal networks by stress. *Front Biosci.* 11:2746–58.2006; [PubMed: 16720347]
39. Magariños AM, McEwen BS. Stress-induced atrophy of apical dendrites of hippocampal CA3c neurons: comparison of stressors. *Neuroscience.* 69:83–8.1995; [PubMed: 8637635]
40. Vyas A, Bernal S, Chattarji S. Effects of chronic stress on dendritic arborization in the central and extended amygdala. *Brain Res.* 965:290–4.2003; [PubMed: 12591150]

41. Vyas A, Pillai AG, Chattarji S. Recovery after chronic stress fails to reverse amygdaloid neuronal hypertrophy and enhanced anxiety-like behavior. *Neuroscience*. 128:667–673.2004; [PubMed: 15464275]
42. Muhammad A, Carroll C, Kolb B. Stress during development alters dendritic morphology in the nucleus accumbens and prefrontal cortex. *Neuroscience*. 216:103–109.2012; [PubMed: 22542675]
43. Anacker C, et al. Neuroanatomic Differences Associated With Stress Susceptibility and Resilience. *Biol Psychiatry*. 79:840–849.2016; [PubMed: 26422005]
44. Christoffel DJ, et al. $\text{I}\kappa\text{B}$ kinase regulates social defeat stress-induced synaptic and behavioral plasticity. *J Neurosci*. 31:314–21.2011; [PubMed: 21209217]
45. Christoffel DJ, Golden SA, Russo SJ. Structural and synaptic plasticity in stress-related disorders. *Rev Neurosci*. 22:535–49.2011; [PubMed: 21967517]
46. Kulkarni VA, Firestein BL. The dendritic tree and brain disorders. *Mol Cell Neurosci*. 50:10–20.2012; [PubMed: 22465229]
47. Grieve SM, Korgaonkar MS, Koslow SH, Gordon E, Williams LM. Widespread reductions in gray matter volume in depression. *NeuroImage Clin*. 3:332–9.2013; [PubMed: 24273717]
48. Koolschijn PCMP, van Haren NEM, Lensvelt-Mulders GJLM, Hulshoff Pol HE, Kahn RS. Brain volume abnormalities in major depressive disorder: A meta-analysis of magnetic resonance imaging studies. *Hum Brain Mapp*. 30:3719–3735.2009; [PubMed: 19441021]
49. Newey SE, Velamoor V, Govek EE, Van Aelst L. Rho GTPases, dendritic structure, and mental retardation. *J Neurobiol*. 64:58–74.2005; [PubMed: 15884002]
50. Nakayama AY, Harms MB, Luo L. Small GTPases Rac and Rho in the Maintenance of Dendritic Spines and Branches in Hippocampal Pyramidal Neurons. *J Neurosci*. 202000;
51. Peck JW, Oberst M, Bouker KB, Bowden E, Burbelo PD. The RhoA-binding protein, rhotillin-2, regulates actin cytoskeleton organization. *J Biol Chem*. 277:43924–32.2002; [PubMed: 12221077]
52. Luo L. Actin Cytoskeleton Regulation in Neuronal Morphogenesis and Structural Plasticity. *Annu Rev Cell Dev Biol*. 18:601–635.2002; [PubMed: 12142283]
53. Camera P, et al. The RhoA-associated protein Citron-N controls dendritic spine maintenance by interacting with spine-associated Golgi compartments. *EMBO Rep*. 9:384–392.2008; [PubMed: 18309323]
54. Chen H, Firestein BL. RhoA Regulates Dendrite Branching in Hippocampal Neurons by Decreasing Cypin Protein Levels. *J Neurosci*. 272007;
55. Sanz E, et al. Cell-type-specific isolation of ribosome-associated mRNA from complex tissues. *Proc Natl Acad Sci*. 106:13939–13944.2009; [PubMed: 19666516]
56. Chandra R, et al. Drp1 Mitochondrial Fission in D1 Neurons Mediates Behavioral and Cellular Plasticity during Early Cocaine Abstinence. *Neuron*. 96:1327–1341.e6.2017; [PubMed: 29268097]
57. Golden SA, Covington HE, Berton O, Russo SJ. A standardized protocol for repeated social defeat stress in mice. *Nat Protoc*. 6:1183–91.2011; [PubMed: 21799487]
58. Ferreira TA, et al. Neuronal morphometry directly from bitmap images. *Nat Methods*. 11:982–4.2014; [PubMed: 25264773]
59. Chandra R, et al. Opposing Role for Egr3 in Nucleus Accumbens Cell Subtypes in Cocaine Action. *J Neurosci*. 35:7927–7937.2015; [PubMed: 25995477]
60. Chandra R, et al. Optogenetic inhibition of D1R containing nucleus accumbens neurons alters cocaine-mediated regulation of Tiam1. *Front Mol Neurosci*. 6:13.2013; [PubMed: 23745104]
61. Subauste MC, et al. Rho family proteins modulate rapid apoptosis induced by cytotoxic T lymphocytes and Fas. *J Biol Chem*. 275:9725–33.2000; [PubMed: 10734125]
62. Hodes GE, et al. Sex Differences in Nucleus Accumbens Transcriptome Profiles Associated with Susceptibility versus Resilience to Subchronic Variable Stress. *J Neurosci*. 35:16362–76.2015; [PubMed: 26674863]
63. Gerfen CR, Paletzki R, Heintz N. GENSAT BAC Cre-Recombinase Driver Lines to Study the Functional Organization of Cerebral Cortical and Basal Ganglia Circuits. *Neuron*. 80:1368–1383.2013; [PubMed: 24360541]

64. Magariños AM, McEwen BS, Flügge G, Fuchs E. Chronic psychosocial stress causes apical dendritic atrophy of hippocampal CA3 pyramidal neurons in subordinate tree shrews. *J Neurosci.* 16:3534–40.1996; [PubMed: 8627386]
65. Chen Y, Dubé CM, Rice CJ, Baram TZ. Rapid loss of dendritic spines after stress involves derangement of spine dynamics by corticotropin-releasing hormone. *J Neurosci.* 28:2903–11.2008; [PubMed: 18337421]
66. Chen Y, et al. Impairment of synaptic plasticity by the stress mediator CRH involves selective destruction of thin dendritic spines via RhoA signaling. *Mol Psychiatry.* 18:485–496.2013; [PubMed: 22411227]
67. Swanson AM, DePoy LM, Gourley SL. Inhibiting Rho kinase promotes goal-directed decision making and blocks habitual responding for cocaine. *Nat Commun.* 8:1861.2017; [PubMed: 29187752]
68. García-Rojo G, et al. The ROCK Inhibitor Fasudil Prevents Chronic Restraint Stress-Induced Depressive-Like Behaviors and Dendritic Spine Loss in Rat Hippocampus. *Int J Neuropsychopharmacol.* 20:336–345.2017; [PubMed: 27927737]
69. Xiao J, et al. Acute Effects of Rho-Kinase Inhibitor Fasudil on Pulmonary Arterial Hypertension in Patients With Congenital Heart Defects. *Circ J.* 79:1342–1348.2015; [PubMed: 25797071]
70. Fukumoto Y, et al. Double-blind, placebo-controlled clinical trial with a rho-kinase inhibitor in pulmonary arterial hypertension. *Circ J.* 77:2619–25.2013; [PubMed: 23912836]

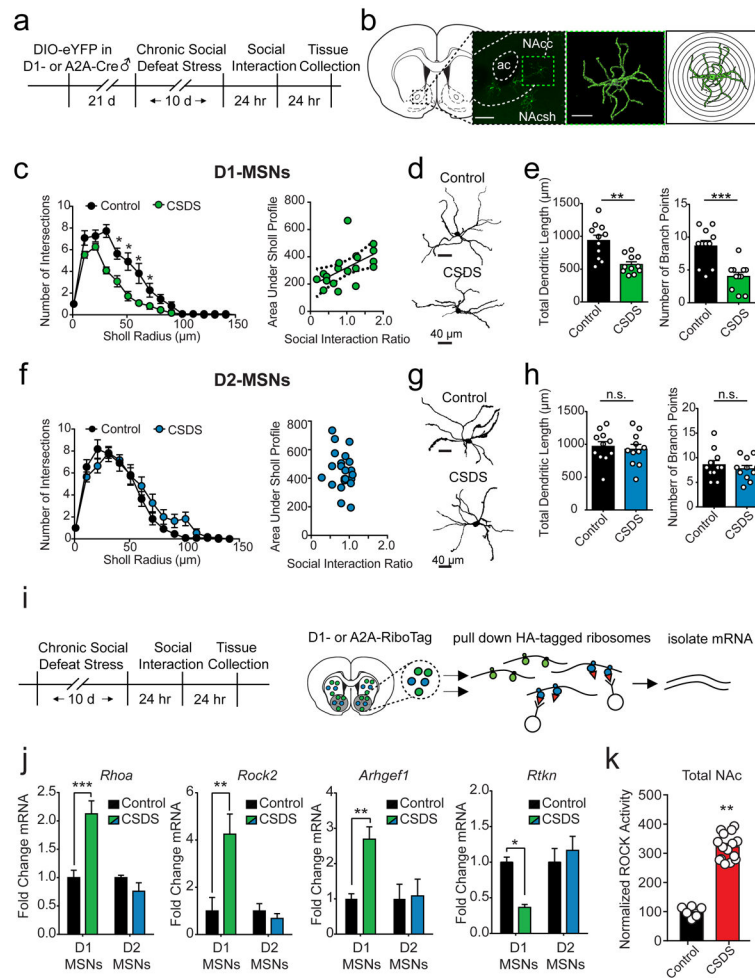


Figure 1. Stress reduces dendritic complexity of NAc D1 MSNs

(a) Experimental timeline. D1 or A2A-Cre mice were injected with AAV-eYFP to label D1- or D2-MSNs prior to chronic social defeat stress (CSDS). (b) Representative image of sparsely labeled MSNs in the NAc, a single MSN after 3D reconstruction, and concentric rings for sholl analysis. (c) Sholl analysis of D1-MSNs from control and CSDS mice ($P < 0.0001$; $n = 11$ cells/group from 12 mice), and area under sholl profile vs social interaction ratio for individual mice. (d) Representative D1-MSNs, (e) total dendritic length, and number of branch points from CSDS and control mice (Length, $P < 0.01$, Branch Points, $P < 0.001$). (f) Sholl analysis of D2-MSNs and area under sholl profile vs social interaction. (g) Representative D2-MSNs, (h) total dendritic length and number of branch points from CSDS and control mice (11 cells/group from 11 mice). (i). Experimental timeline and schematic of RiboTag method for isolation of ribosome-associated mRNA from MSN subtypes. Cre-dependent HA-tags (red) are expressed on ribosomes in MSN subtypes. RNA was purified following ribosome immunoprecipitation with anti-HA coated magnetic beads. (j) *Rhoa* pathway genes are altered in D1-MSNs of CSDS mice (D1: *Rhoa* $P = 0.0008$, *Rock2* $P = 0.0031$, *Arhgef1* $P = 0.0067$, *Rtkn* $P = 0.0150$, 4–6 samples/group, 4 mice pooled/sample). (k) Rho-kinase (ROCK) activity as a percent of control in total NAc lysates from control and CSDS mice ($P < 0.0001$, $n = 6–15$ /group).

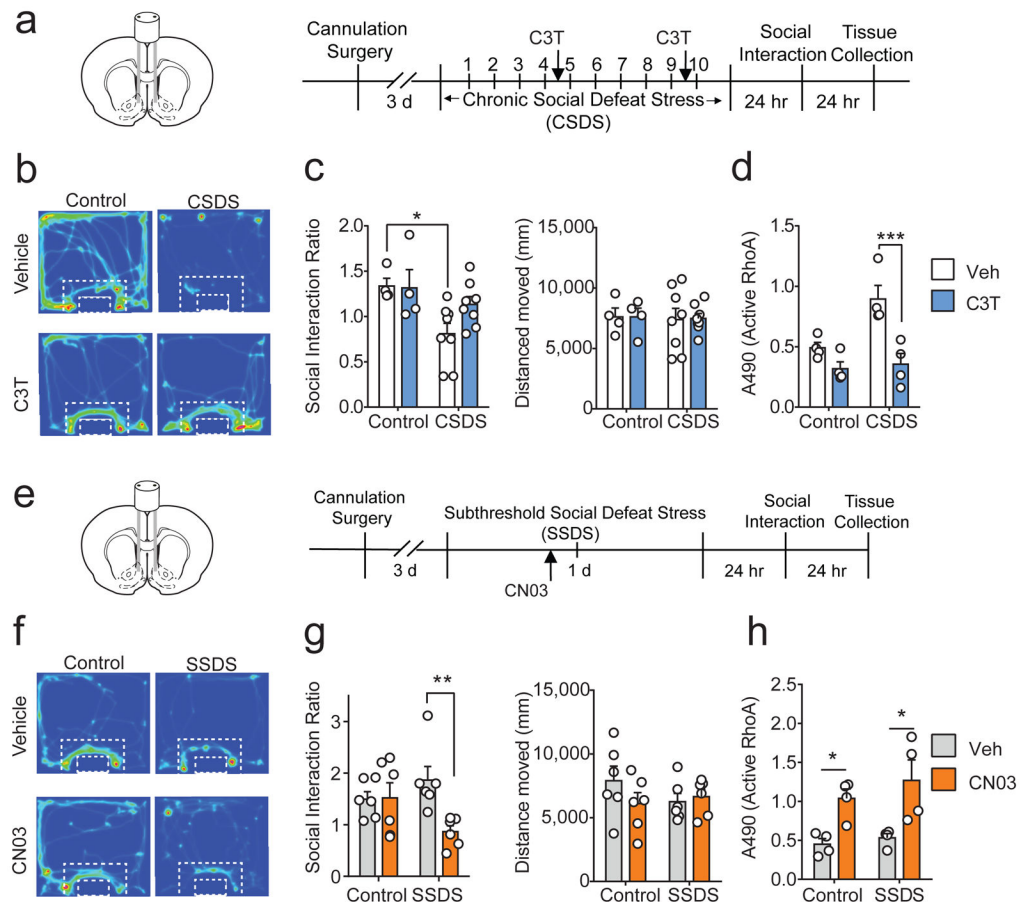


Figure 2. RhoA in the NAC controls depressive outcomes to stress

(a) Experimental timeline and schematic of cannula placement in the NAC. Mice were treated with intra-NAC vehicle or 10 ug/mL Rho Inhibitor C3T (500 nL/side) 4 hr prior to day 5 and 10 of CSDS. (b) Heat maps showing mouse movement within the social interaction arena during the presence of a novel mouse. Warm colors indicate more time is spent in an area and cool colors indicate less time. (c) Effect of NAC Rho inhibition on social avoidance ($P=0.0170$, $n=4-8$ /group) and locomotion ($P>0.05$), and (d) activated RhoA after CSDS ($P=0.0010$) (e) Experimental timeline and schematic of cannula placement. Mice were treated with intra-NAC vehicle or 10 ug/mL Rho activating compound CN03 4 hours prior to SSDS. (f) Heat maps showing mouse movement within social interaction arena during the presence of a novel mouse. (g) Effect of Rho activation on social interaction ($P=0.0082$, $n=6$ /group) and locomotion ($P>0.05$), and (h) activated RhoA (Control $P=0.0364$, SSDS $P=0.0101$)

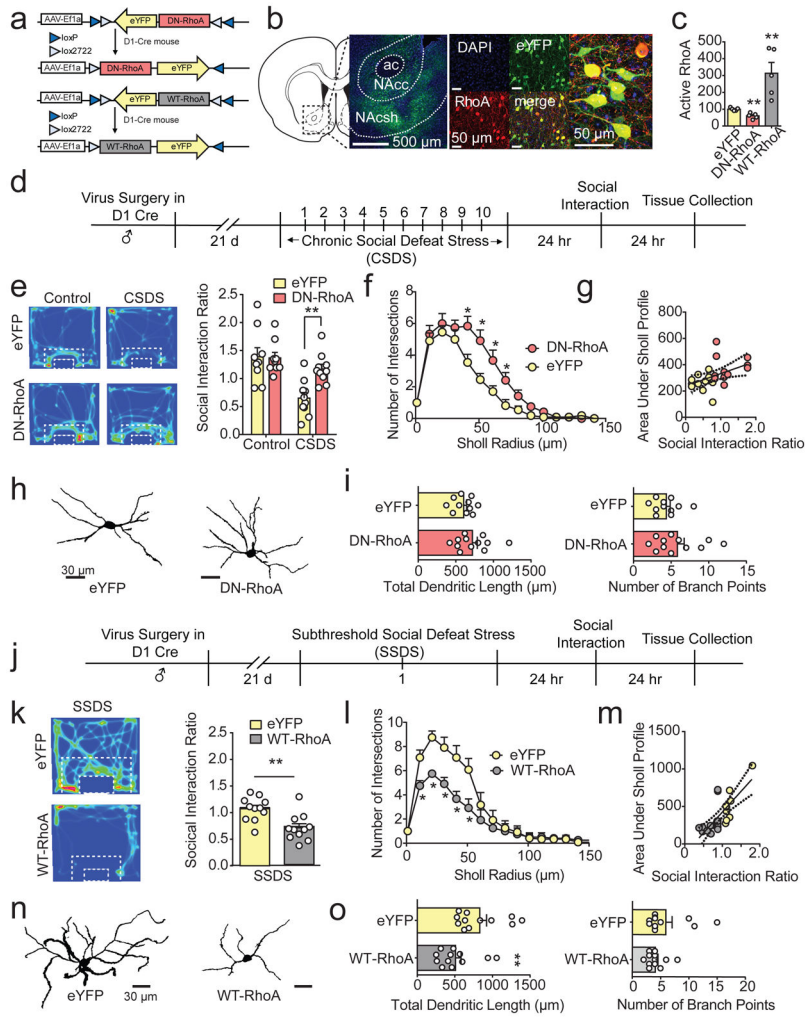


Figure 3. RhoA in D1-MSNs alters dendritic complexity and depressive outcomes to stress (a) Schematics of the double-floxed, inverted, open reading frame Cre-dependent AAV vectors for overexpression of dominant negative (RhoA-T19N; DN) or wildtype (WT) RhoA. (b) Virus injection site in the NAc showing native eYFP fluorescence (green) and DAPI (blue), and immunolabeling for eYFP (green) and RhoA (red). (c) Activated RhoA as percent of eYFP (vs DN, $P=0.0016$, vs WT $P=0.0112$, $n=5$ /group) (d). Experimental timeline for RhoA inhibition during CSDS. Male D1-Cre mice were bilaterally injected with DN-RhoA or eYFP vectors prior to CSDS. (e) Heat maps showing mouse movement in the social interaction arena with novel mouse present. Effect of DN-RhoA on social avoidance in CSDS ($P=0.0042$, $n=9-10$ /group) and control mice. (f) Sholl analysis of D1-MSNs ($P<0.05$, $n=11$ cells/group from 11 total mice), (g) area under sholl profile vs social interaction ratio in individual mice (slope, $P=0.0238$), (h) representative D1-MSNs and (i) total dendritic length ($P=0.1445$) and number of branch points ($P=0.1783$) from CSDS mice expressing eYFP and DN-RhoA. (j) Experimental timeline for RhoA Activation during SSDS. Male D1-cre mice were injected with WT-RhoA or eYFP vectors. (k) Heatmaps and social interaction behavior in SSDS mice expressing eYFP or WT-RhoA ($P=0.0021$, $n=11$ /group) (l) Sholl analysis ($P<0.05$, $n=12$ cells/group from 13 total mice), (m) area under sholl

profile vs social interaction for individual mice (slope, $P < 0.0001$) (**n**) representative D1-MSNs and (**o**) total dendritic length ($P = 0.0116$) and number of branch points ($P = 0.1514$) from SSDS mice expressing eYFP and WT-RhoA

Author Manuscript

Author Manuscript

Author Manuscript

Author Manuscript

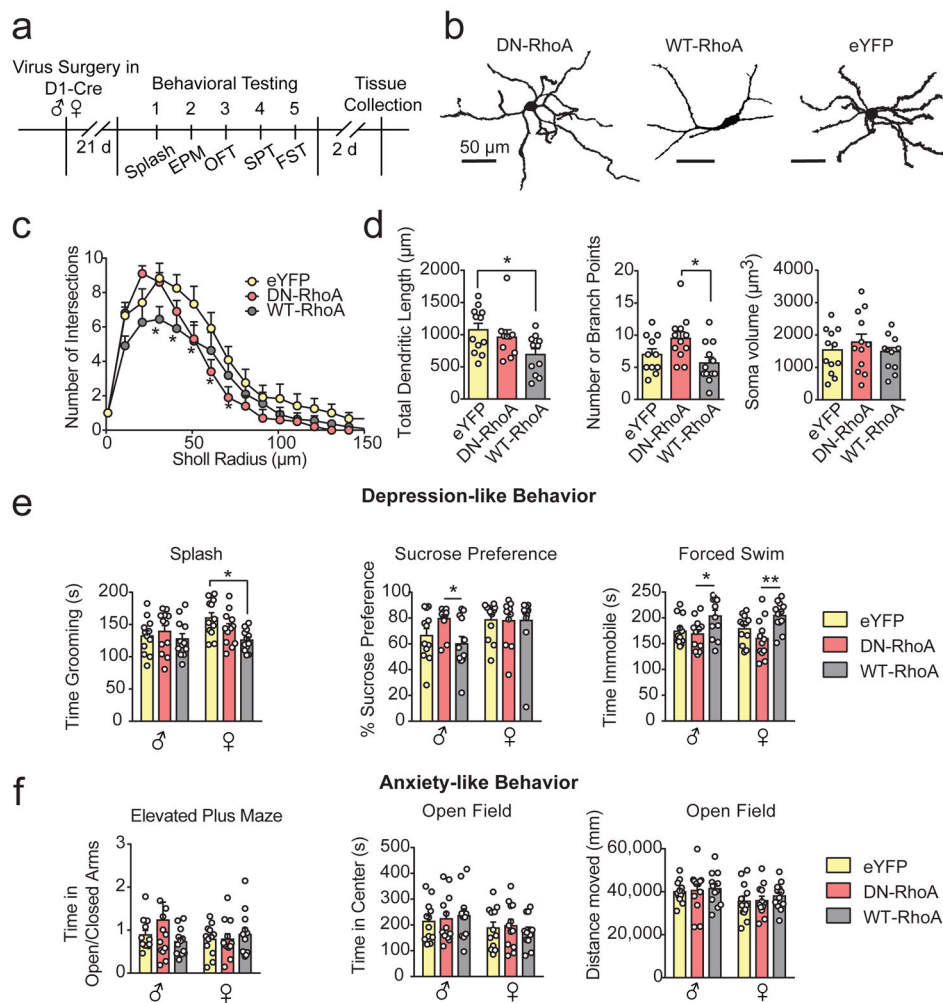


Figure 4. RhoA in D1-MSNs alters dendritic complexity and enhances depressive behaviors in stress-naïve mice

(a) Experimental timeline. Male and female mice D1-Cre mice were injected bilaterally with DN-RhoA, WT-RhoA, or eYFP vectors prior to 5 days of behavioral testing. (b) Representative D1-MSNs (c) sholl analysis ($P < 0.0001$, 10–12 cells/group from 17 mice), (d) total dendritic length ($P = 0.0005$), number of branch points ($P = 0.0102$), and soma volume ($P > 0.05$) from stress-naïve mice expressing DN-RhoA, WT-RhoA, or eYFP. (e) WT-RhoA decreases time spent grooming in the splash test (females; $P = 0.0084$) sucrose preference (males, $P = 0.0254$), and increases time spent floating in the forced swim test (Male, $P = 0.0294$; Female, $P = 0.0035$, $n = 12$ mice/sex/group) (f). D1-MSN RhoA manipulations do not impact anxiety-like behavior in the elevated plus maze or open field, nor do they alter locomotion ($P > 0.05$, $n = 12$ mice/sex/group).

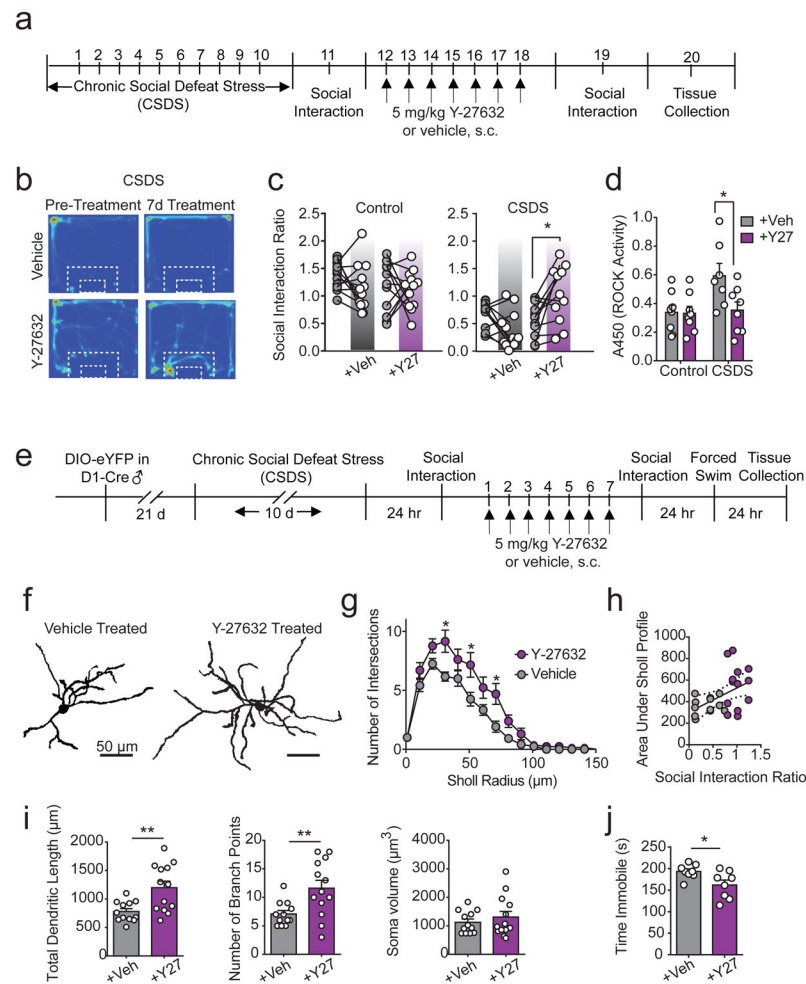


Figure 5. Rho-kinase inhibition acts as an antidepressant treatment and reverses dendritic atrophy

(a). Experimental timeline. After 10 days of CSDS and social interaction testing, mice were treated with vehicle (veh) or 5 mg/kg Rho-kinase (ROCK) inhibitor Y-27632 (Y27) once daily for 7 days, then re-tested for social interaction. (b). Heatmaps showing mouse movement in the social interaction arena with novel mouse present before and after 7 days treatment with vehicle or ROCK inhibitor. (c) Effect of 7 days treatment with ROCK inhibitor on social interaction behavior in control and CSDS mice ($n=12$ mice/group; CSDS +Y27632, $P=0.0182$) (d) Effect of vehicle or ROCK inhibitor treatment on ROCK Activity. (e) Experimental timeline for assessing dendritic complexity. Male D1-Cre mice were injected with a low-titer AAV-eYFP to label D1-MSNs prior to CSDS. Mice were tested for social interaction, treated for 7 days with 5 mg/kg Y-27632, then underwent social interaction and forced-swim testing. (f) Representative D1-MSNs (g) sholl analysis, (12–13 cells/group from 9 mice) (i) area under the sholl profile vs social interaction ratio for individual mice (Slope $P=0.0183$), (h) total dendritic length ($P=0.0041$), number of branch points ($P=0.0076$), and soma volume of D1-MSNs from CSDS mice treated with vehicle or

Y-27632. (j) Effect of Y27 treatment on immobility time in veh and y27 treated CSDS mice ($P=0.0265$, $n=8$ mice/group).

Author Manuscript

Author Manuscript

Author Manuscript

Author Manuscript